

Electronic Supplementary Material (ESI) for Dalton Transactions.

This journal is © The Royal Society of Chemistry 2023

Supplementary Information

Accelerating the reaction kinetics of $\text{Ni}_{1-x}\text{O}/\text{Ni(OH)}_2/\text{NF}$ by defect engineering for urea-assisted water splitting

Yuan Rui,^a Zong Li,^a Miao hui Wang,^a Yunxia Liu,^{,b} Haiping Lin,^a Peipei Huang^{*,a} and Qing Li^{*,a}*

^aSchool of Physics and Information Technology, Shaanxi Normal University, Xi'an, 710119, P. R. China

^bSchool of Chemistry and Chemical Engineering, Northwestern Polytechnical University, Xi'an, 710072, P. R. China.

*Corresponding author: yxliu@nwpu.edu.cn; huangpeipei@snnu.edu.cn; liqing@snnu.edu.cn;

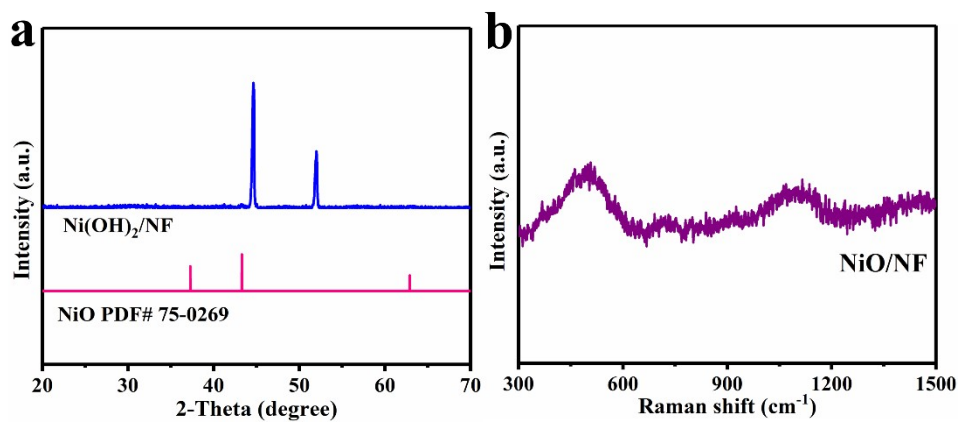


Fig. S1 (a) The XRD pattern of Ni(OH)₂/NF. (b) The Raman spectrum of NiO/NF.

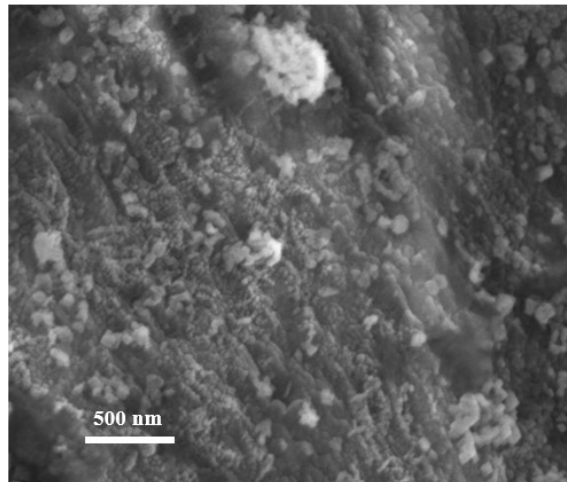


Fig. S2 The SEM image of Ni(OH)₂/NF.

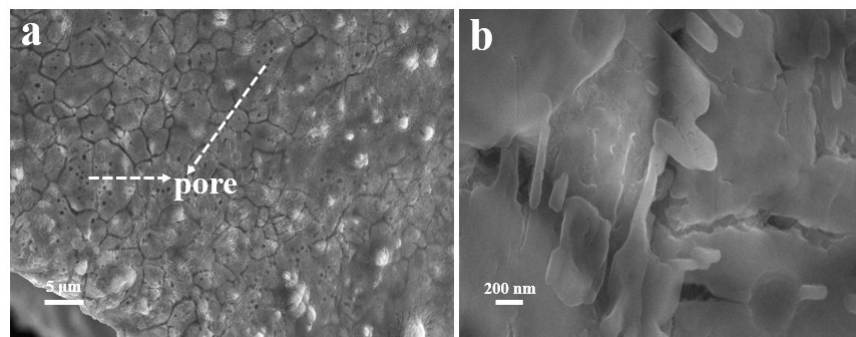


Fig. S3 SEM images at different magnifications of treated nickel foam (a, b).

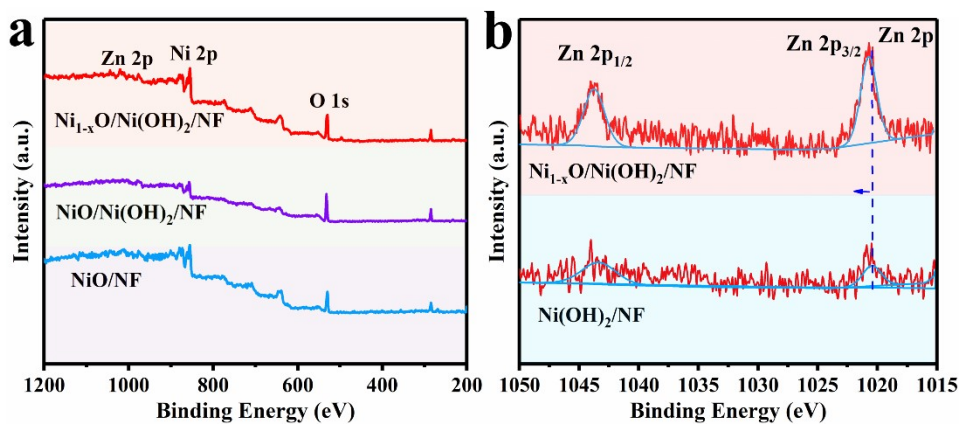


Fig. S4 (a) XPS survey spectra of NiO/NF , $\text{NiO}/\text{Ni}(\text{OH})_2/\text{NF}$ and $\text{Ni}_{1-x}\text{O}/\text{Ni}(\text{OH})_2/\text{NF}$. (b) High-resolution Zn 2p XPS spectra of $\text{Ni}_{1-x}\text{O}/\text{Ni}(\text{OH})_2/\text{NF}$ and $\text{Ni}(\text{OH})_2/\text{NF}$.

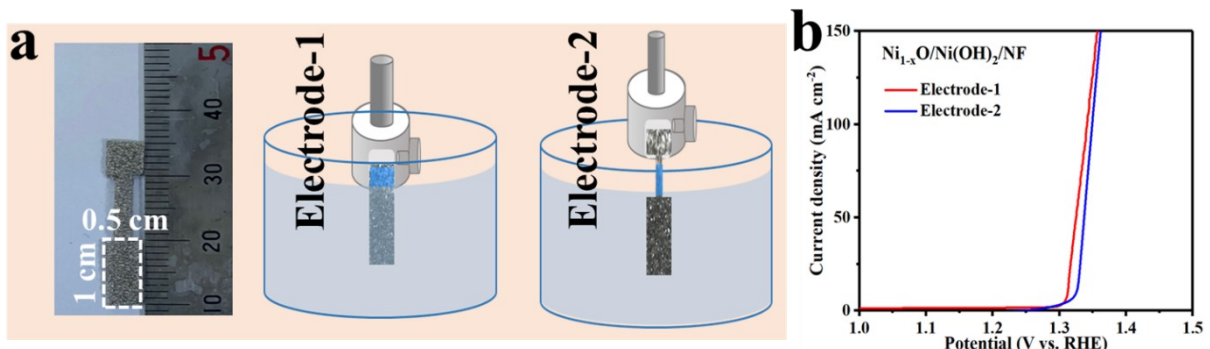


Fig. S5 (a) A representative digital photograph of the working electrode with a specifically designed shape. The schematic diagram illustrates the application of the working electrode in UOR performance measurement without (electrode-1) and with (electrode-2) the special shape. (b) LSV curves acquired with electrode-1 and electrode-2 loading with $\text{Ni}_{1-x}\text{O}/\text{Ni}(\text{OH})_2/\text{NF}$.

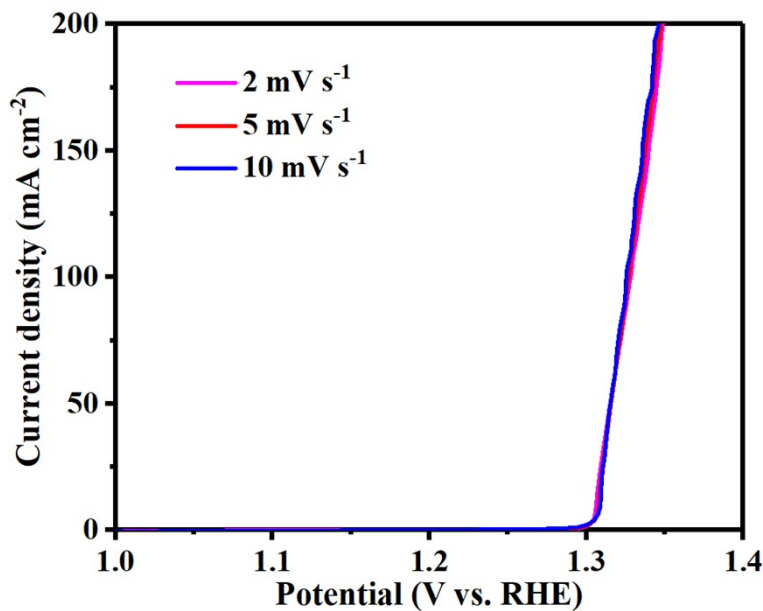


Fig. S6 UOR polarization curves of $\text{Ni}_{1-x}\text{O}/\text{Ni}(\text{OH})_2/\text{NF}$ in 1 M KOH with 0.33 M urea at scanning rates of 10 mV s^{-1} , 5 mV s^{-1} and 2 mV s^{-1} , respectively.

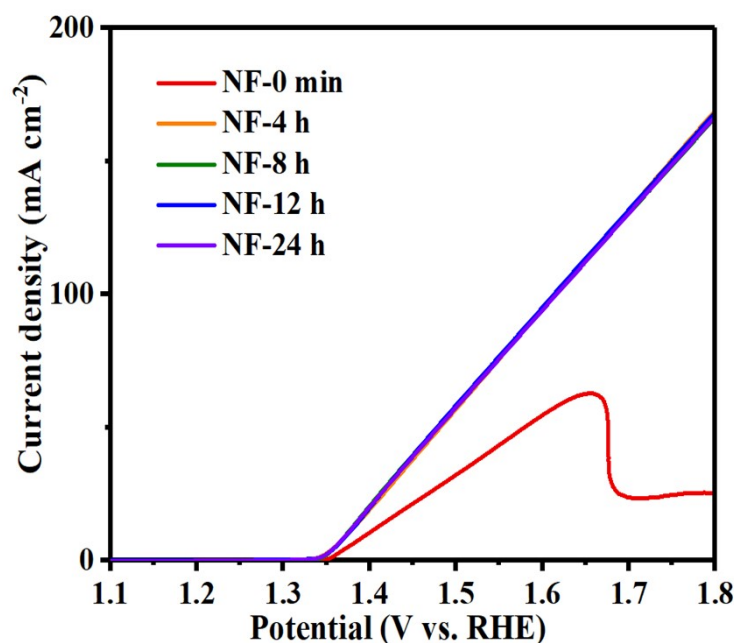


Fig. S7 LSV curves of NF with different acid etching time durations.

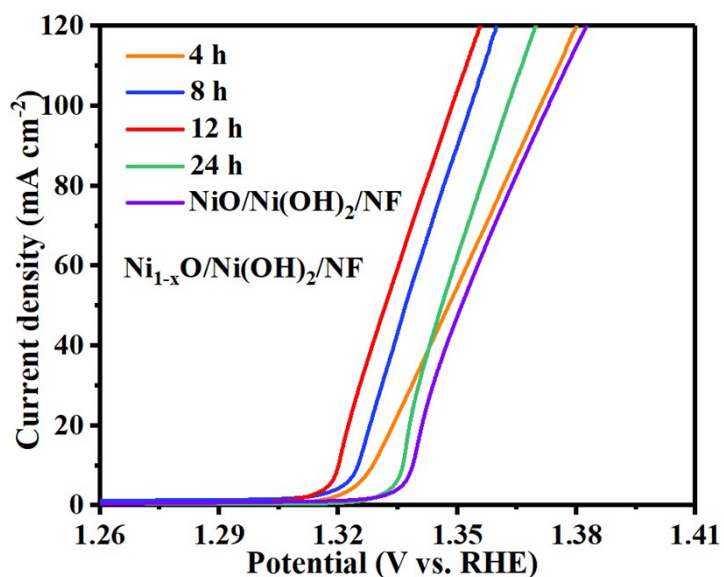


Fig. S8 LSV curves of $\text{Ni}_{1-x}\text{O}/\text{Ni(OH)}_2/\text{NF}$ with different acid etching times and $\text{NiO}/\text{Ni(OH)}_2/\text{NF}$.

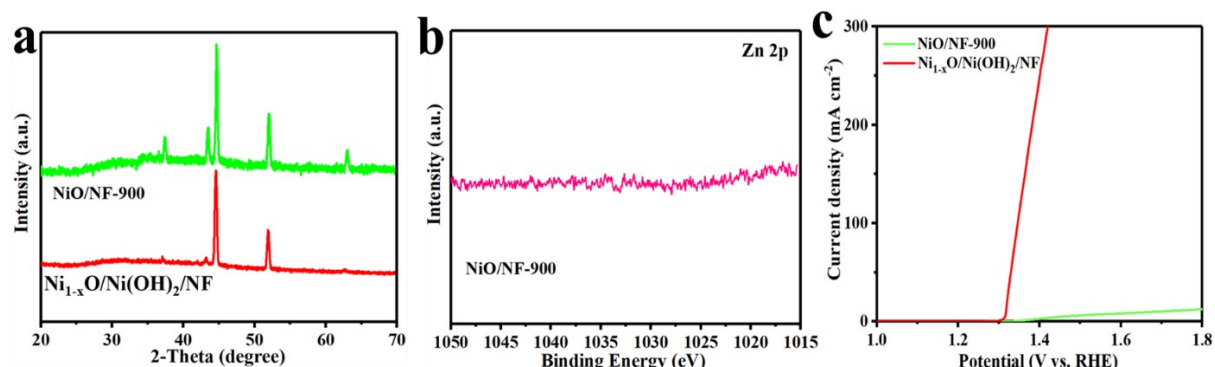


Fig. S9 (a) XRD patterns of NiO/NF-900 and $\text{Ni}_{1-x}\text{O}/\text{Ni(OH)}_2/\text{NF}$. (b) The high-resolution Zn 2p XPS spectrum of NiO/NF-900. (c) LSV curves of NiO/NF-900 and $\text{Ni}_{1-x}\text{O}/\text{Ni(OH)}_2/\text{NF}$.

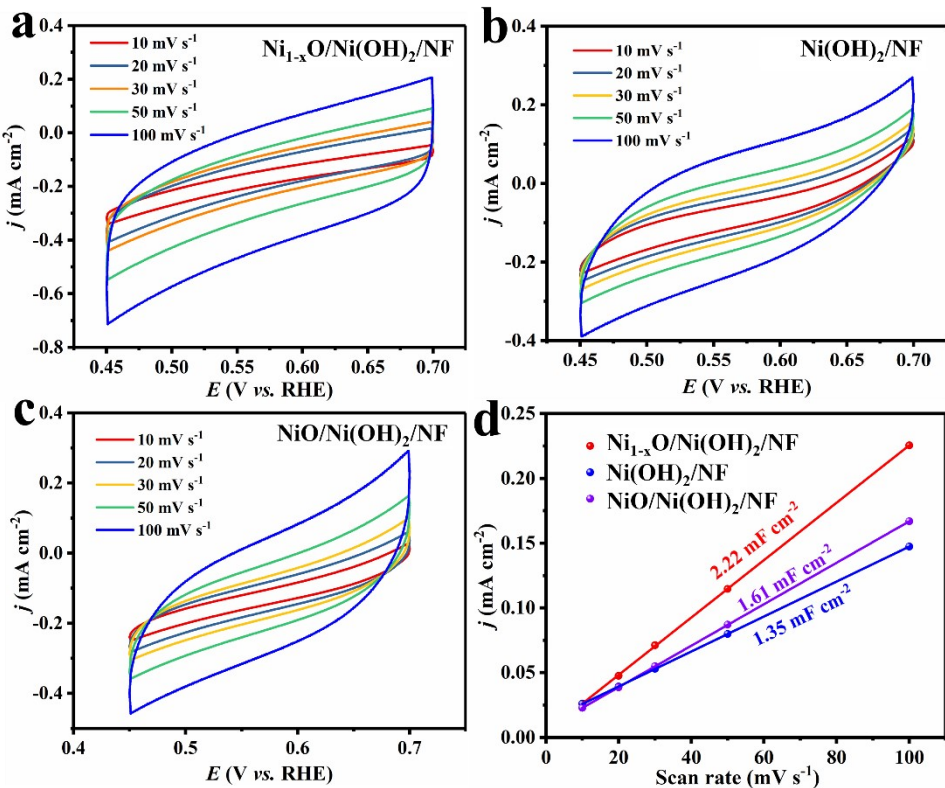


Fig. S10 CV curves for (a) $\text{Ni}_{1-x}\text{O}/\text{Ni(OH)}_2/\text{NF}$, (b) $\text{Ni(OH)}_2/\text{NF}$, and (c) $\text{NiO}/\text{Ni(OH)}_2/\text{NF}$ at different scan rates in the non-faradaic potential region. (d) Linear relationships between the capacitive current and the scan rate of catalysts.

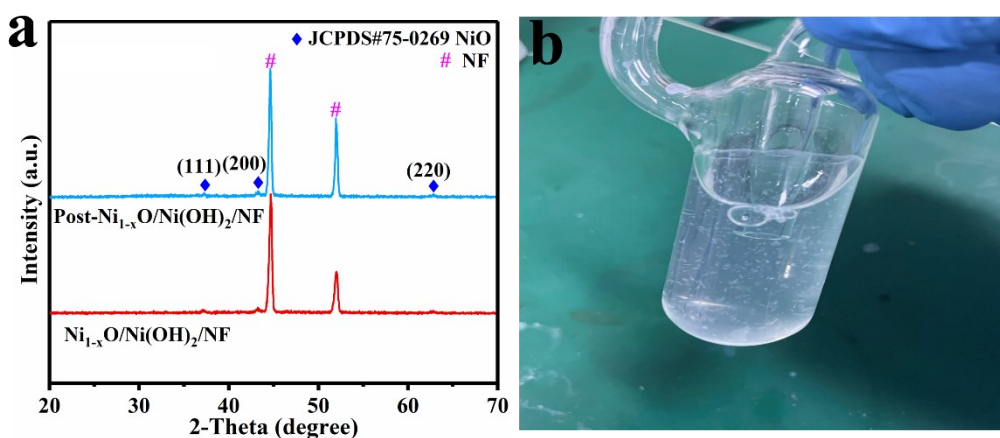


Fig. S11 XRD patterns of the Post- $\text{Ni}_{1-x}\text{O}/\text{Ni(OH)}_2/\text{NF}$ and $\text{Ni}_{1-x}\text{O}/\text{Ni(OH)}_2/\text{NF}$. (b) The digital photograph during the chronopotentiometry test of $\text{Ni}_{1-x}\text{O}/\text{Ni(OH)}_2/\text{NF}$, in which the saturated Ca(OH)_2 solution became turbid, signifying the production of CO_2 .¹

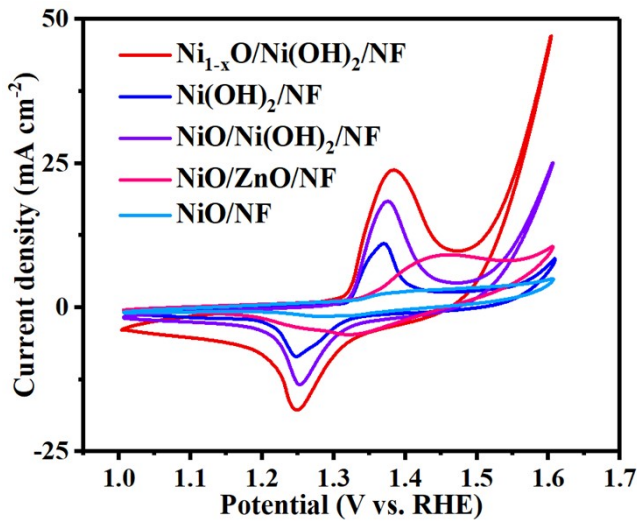


Fig. S12 CV curves of $\text{Ni}_{1-x}\text{O}/\text{Ni}(\text{OH})_2/\text{NF}$, $\text{Ni}(\text{OH})_2/\text{NF}$, $\text{NiO}/\text{Ni}(\text{OH})_2/\text{NF}$, $\text{NiO}/\text{ZnO}/\text{NF}$ and NiO/NF in 1 M KOH with 10 mV s^{-1} .

Ni^{2+} sites are firstly electrochemically oxidized to high-valent Ni^{3+} species in the forward scanning, and Ni^{3+} species then chemically oxidize urea molecules with themselves being reduced back to Ni^{2+} . As shown in Fig. S12, the CV curve of $\text{Ni}_{1-x}\text{O}/\text{Ni}(\text{OH})_2/\text{NF}$ exhibits the largest oxidation peak, suggesting most Ni^{3+} sites are generated in $\text{Ni}_{1-x}\text{O}/\text{Ni}(\text{OH})_2/\text{NF}$ and conducive to a great UOR performance.

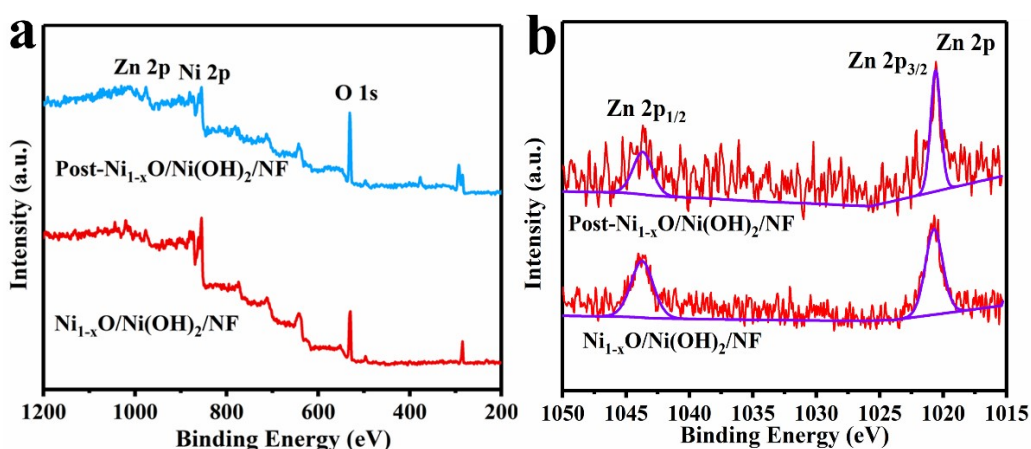


Fig. S13 (a) XPS survey spectra and (b) high-resolution XPS spectra of Zn 2p for $\text{Ni}_{1-x}\text{O}/\text{Ni}(\text{OH})_2/\text{NF}$ and Post- $\text{Ni}_{1-x}\text{O}/\text{Ni}(\text{OH})_2/\text{NF}$.

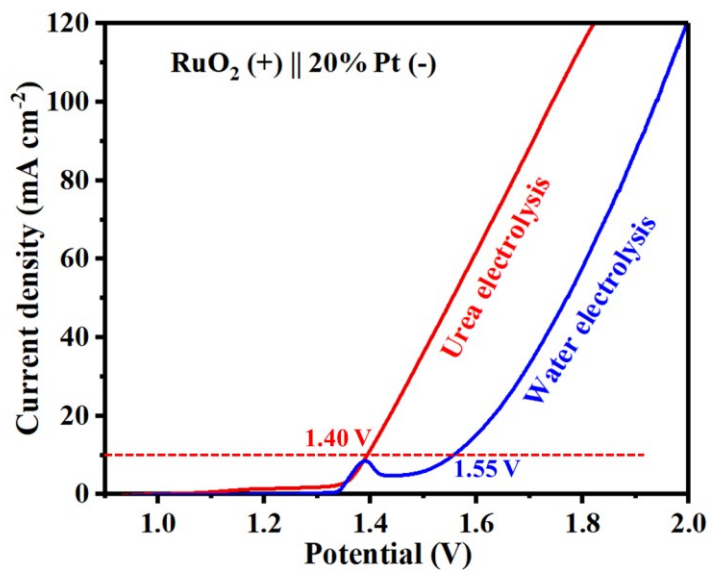


Fig. S14 Two-electrode polarization curves for water splitting and urea splitting of commercial $\text{RuO}_2 (+) \parallel 20\% \text{ Pt/C} (-)$.

Table S1. Element Zn, Ni and O contents of $\text{Ni}_{1-x}\text{O}/\text{Ni(OH)}_2/\text{NF}$ with different acid etching times.

Catalysts	Element	Atomic%*
4 h	Ni	28.36
	Zn	4.94
	O	66.70
8 h	Ni	28.32
	Zn	3.51
	O	68.17
12 h	Ni	25.44
	Zn	2.88
	O	71.68
24 h	Ni	26.92
	Zn	1.55
	O	71.53
Post- $\text{Ni}_{1-x}\text{O}/\text{Ni(OH)}_2/\text{NF}$	Ni	21.90
	Zn	2.72
	O	75.38

*These values were estimated by XPS.

Table S2. Comparison of UOR performances of $\text{Ni}_{1-x}\text{O}/\text{Ni(OH)}_2/\text{NF}$ with recent reported electrocatalysts.

Catalysts	Potential (vs.	Tafel slope	Reference
	RHE)	(mV dec ⁻¹)	
$\text{Ni}_{1-x}\text{O}/\text{Ni(OH)}_2/\text{NF}$	1.317@10 1.346@100	18.7	This work
Ir/NiPS_3	1.36@10	21.1	<i>Nat. Communt.</i> 2024 , 15, 2851.
$\text{Ni(OH)}_2/\text{g-C}_3\text{C}_4$	1.361@10	/	<i>Small</i> 2024 , 2401053.
$\text{LaNiO}_3-\text{NiO}$	1.34@10	39.87	<i>ACS Materials Lett.</i> 2024 , 6, 1029-1041.
$\text{Pt}-\text{Ni(OH)}_2@\text{Ni-CNFs-2}$	1.363@10	13.4	<i>Energy Environ. Sci.</i> , 2024 , 17, 1984-1996.
pt-NFS	1.37@10	49.87	<i>Small Methods</i> 2024 , 2301434.
$\text{V-Co}_2\text{P}_4\text{O}_{12}/\text{CC}$	1.33@10	50	<i>Adv. Funct. Mater.</i> 2024 , 2313974.
$\text{CF}@\text{CoOS-2}$	1.36@10	155	<i>Small</i> 2024 , 2310112.
$\text{a-RuO}_2/\text{NiO}$	1.334@10	34.8	<i>ACS Nano</i> 2024 , 18, 1214-1225.
NiB_x	1.40@100	22.8	<i>Adv. Funct. Mater.</i> 2024 , 2411011.
Ni SAs-NC	1.39@10	42	<i>Appl. Catal. B. Environ</i> 2022 , 310, 121352.
$\text{NiO/CuO}@ \text{CuM}$	1.35@10	32.2	<i>Nano Energy</i> 2023 , 115, 108714.
$\text{Cu}_{0.5}\text{Ni}_{0.5}/\text{NF}$	1.33@10	22.77	<i>Small</i> 2023 , 19, 2300959.
$\text{Co/CoSe}_2@\text{CNx}$	1.34@10	-	<i>J. Mater. Chem. A</i> , 2023 , 11, 5179-5187.
$\text{WM-Ni}_{0.99}\text{Co}_{0.01}(\text{OH})_2$	1.37@10	31	<i>Energy Environ. Mater.</i> 2023 , 0, e1257.
$\text{Ni/W}_5\text{N}_4/\text{NF}$	1.34@10	35.8	<i>Appl. Catal. B. Environ.</i> 2023 , 323, 122168.
$\text{Ni}_{0.05}/\text{CW}$	1.36@10	20.93	<i>J. Energy Chem.</i> 2023 , 76, 566-575.
Cu-NiFe LDH	1.35@onset	26	<i>Adv. Energy Mater.</i> 2024 , 2403004.
Ni(OH)S/NF	1.34@10	-	<i>Appl. Catal. B. Environ.</i> 2022 , 312, 121389.
Rh/NiV-LDH	1.33@10	36	<i>Sci. Bulletin</i> 2022 , 67, 1763-1775.

Table S3. Comparison of urea electrolysis performances of $\text{Ni}_{1-x}\text{O}/\text{Ni(OH)}_2/\text{NF} \parallel 20\% \text{ Pt/C}$ with that of previously reported catalysts.

Catalysts	Current density (mA/cm ⁻²)	Potential(V)	Reference
Ni_{1-x}O/Ni(OH)₂/NF 20% Pt/C	10	1.379	This work
YNi-10 Pt/C	10	1.47	ACS Appl. Mater. Interfaces 2024 , 16, 50937–50947.
V-Ni(OH) ₂ Pt foil	10	1.50	Adv. Funct. Mater. 2022 , 2209698
WN/Ni ₃ N Pt/C	10	1.38	Adv. Energy Mater. 2023 , 13, 2302452.
NiFe-F-4 Pt/C	50	1.65	J. Colloid Interf. Sci. 2022 , 615, 309-317.
CrCoNiFe Pt/C	10	1.485	J. Mater. Sci. Technol. 2024 , 203, 97-107.
aNi-cys (+) Pt/C (-)	10	1.41	J. Colloid Interf. Sci. 2025 , 679, 1141-1149.
CoS-2 Pt/C	10	1.56	Small 2024 , 20, 2310112.
Mo-FeNi LDH Pt/C	10	1.38	Small 2024 , 20, 2305877.
Ni/MNO-10 Pt/C	10	1.45	Small Struct. 2023 , 4, 2300212.
FeNi-OH/Co(OH) ₂ /NF Pt/C	10	1.44	Appl. Surf. Sci. 2024 , 670, 160649.

REFERENCE

- 1 Z. Ji, Y. Song, S. Zhao, Y. Li, J. Liu and W. Hu, ACS Catal., 2021, **12**, 569-579.